Performance of Successive Reference Pose Tracking vs Smith Predictor Approach for Direct Vehicle Teleoperation Under Variable Network Delays

Jai Prakash [ORCID], Michele Vignati [ORCID], *Member, IEEE*, and Edoardo Sabbioni [ORCID]

Abstract—Vehicle teleoperation holds potential applications as a fallback solution for autonomous vehicles, remote delivery services, hazardous operations, etc. However, network delays and limited situational awareness can compromise teleoperation performance and increase the cognitive workload of human operators. To address these issues, we previously introduced the novel successive reference pose tracking (SRPT) approach, which transmits successive reference poses to the vehicle instead of steering commands. This article compares the stability and performance of SRPT with Smith predictor-based approach for direct vehicle teleoperation in challenging scenarios. The Smith predictor approach is further categorized, one with Lookahead driver and second with Stanley driver. Simulations are conducted in a Simulink environment, considering variable network delays (250–350 ms) and different vehicle speeds (14–26 km/h), and include maneuvers such as tight corners, slalom, low-adhesion roads, and strong crosswinds. The results show that the SRPT approach significantly improves stability and reference tracking performance, with negligible effect of network delays on path tracking. Our findings demonstrate the effectiveness of SRPT in eliminating the detrimental effect of network delays in vehicle teleoperation.

Index Terms—Vehicle teleoperation, remote driving, network delay, latency, time-delay, successive reference pose tracking (SRPT), NMPC, Simulink, Smith predictor, Wireless network communication.

NOMENCLATURE

NMPC	Nonlinear model predictive control.
SRPT	Successive reference pose tracking.
RHIS	Remote human input system.
AD	Autonomous driving.
ODD	Operational Design Domain.
FWD	Front wheel drive.
IMU	Inertial measurement unit.
τ	round trip network delay.
τ_1	Uplink delay part of the round trip delay.
τ_2	Downlink delay part of the round trip delay.
k_1, k_2	Constants for the Lookahead driver model.
k	Constant for the Stanley driver model.
V_x	Vehicle longitudinal speed.
Δy	Cross-track error.
δ	Steer angle.
ψ	Vehicle heading angle.
X_{Ref}	Reference pose.
CG	Center of gravity of the vehicle.
l_F	longitudinal distance between front axle and CG.
L	Vehicle wheelbase.
R	Instantaneous radius of curvature.
s	Distance along track length.
L_{ind}	Lookahead distance for reference-pose driver model.
P_B^A	Relative pose of A with respect to B.
$\Delta t_{Horizon}$	Time horizon for NMPC prediction.
μ	Road adherence coefficient.

I. INTRODUCTION

AUTOMATED vehicles (AVs) have garnered increasing attention as a potential solution for future mobility. However, the deployment of AVs is still hindered by various difficulties and edge cases that have yet to be fully resolved. Teleoperation has emerged as a backup plan for AVs, offering a way to remotely support an AV when it reaches the limits of its operational design domain (ODD). Teleoperation is the remote control of a device or a vehicle from a distance. This can be done using either wired communication or wireless communication. Here the vehicle is a mobile robot that can be controlled remotely, typically wirelessly. The use of teleoperation technology is to offer a secure and effective method to get over these restrictions anytime an AD function hits the limits of its ODD. The AV can resume its voyage in full automation after it has been returned to its nominal ODD [1]. Vehicle teleoperation has the potential to also revolutionize various industries, such as autonomous taxi service, industrial equipment teleoperation, disaster response, and military operations.

Despite having great potential, vehicle teleoperation is currently facing various challenges, such as problems with human-machine interaction, limited situational awareness, network latency, and control loop instability. Although the challenges are significant, we are primarily focusing on reducing the detrimental impact of network latency. By doing so, we are
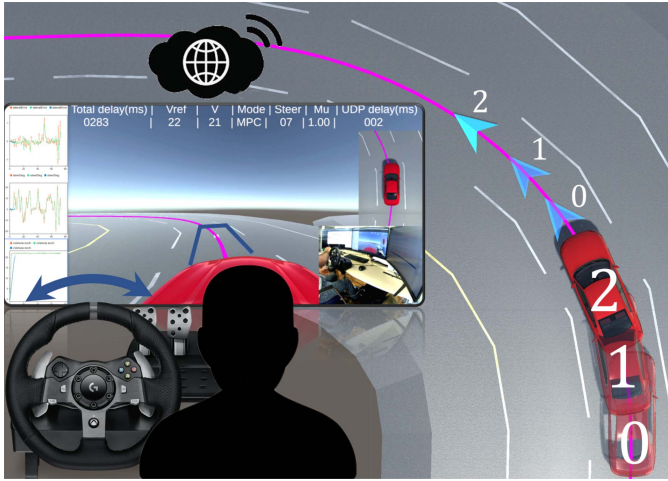
Fig. 1. Pictorial representation of SRPT approach for direct vehicle teleoperation. The remote vehicle receives successive reference poses as it moves forward.
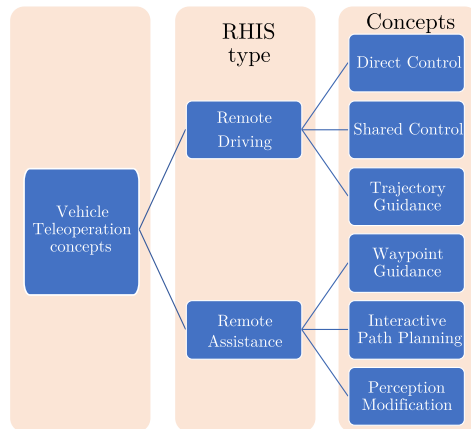

Fig. 2. Vehicle teleoperation concepts in which the human operator is actively involved [1], [2], [3].

aiming to improve the stability of the control loop, which in turn will enhance the safety and effectiveness of teleoperation systems, and ultimately help to achieve more reliable and efficient teleoperation of vehicles.

Daniel Bogdoll et al. [2] proposed a taxonomy for Remote Human Input Systems (RHIS) for vehicle teleoperation based on intervention levels of human operators. It broadly categorizes RHIS approaches into remote driving, remote assistance, and remote monitoring. This classification aligns with the classification of remote operations of vehicles by Oscar Amador et al. [3]. Further refining the remote driving category, Domagoj Majstorovic et al. [1] distinguished between direct control, shared control, and trajectory guidance. They also classified remote assistance techniques into waypoint guidance, interactive path planning, and perception modification. Fig. 2 shows the vehicle teleoperation concepts in which human operator is actively involved.

The time delays in vehicle teleoperation tasks reduce the accuracy and speed at which human operators can perform a remote task [4], [5]. Significant delays can cause overcorrection

by the operator, resulting in oscillations that impair teleoperation performance and may even destabilize the control loop [6], [7]. Direct control [8], [9], [10], [11], [12], [13], [14], [15] approach in vehicle teleoperation involves the operator viewing sensor data and sending control signals like steering and throttle, but it suffers from reduced situational awareness and transmission latency. Shared control [16], [17], [18], [19], [20], [21] has a shared controller inside the vehicle that assesses operator commands to avoid collisions, improving safety but still suffering from latency. Trajectory guidance [22], [23], [24], [25], [26] involves the vehicle following a path and speed profile generated by the operator without being affected by network latency, although real-time profile generation is unfeasible. Interactive path planning [27], [28] uses the vehicle's perception module to calculate optimal paths, which the operator confirms to follow, bypassing network latency but requiring a functional set of AD perception module. Perception modification [29] involves the operator identifying false-positive obstacles to support the AD perception module, which largely depends on the availability of AD perception module.

Our work on SRPT vehicle teleoperation stands out as it strengthens the direct control concept. Direct control concept doesn't rely on the automation and perception modules of autonomous vehicles. Unlike other teleoperation concepts that depend on the perception module, direct control offers independence, acting as a fallback option for autonomous vehicles. The perception module, while essential for autonomous driving, has drawbacks such as limited performance in adverse weather, vulnerability to sensor interference, processing time, computational load, and other challenges. In scenarios where the perception module fails, other teleoperation methods become infeasible. By focusing on enhancing direct control, our SRPT approach aims to overcome these limitations and provide a more dependable vehicle teleoperation solution.

A. Related Work

Direct control - In response to the rising interest in remote operation systems, Hofbauer et al. [30] developed a system that enables direct control interaction with a vehicle during teleoperation in the CARLA driving simulator. To address the lack of publicly available software for remote driving functionalities, Schimpe et al. [31] contributed by releasing an open-source software implementation. This software is designed for quick and flexible deployment across various automotive vehicles and has been successfully used in projects like UNICARagil [32] and 5GCroCo [33]. Chucholowski et al. [11] evaluated the "Frame Prediction" method for teleoperating road vehicles, using a single-track vehicle dynamic model to predict vehicle positions [34]. Tang et al. [12] introduced the Free Corridor for ensuring a safe end state in case of connection failure. Graf et al. [13] combined these ideas to create the "Predictive Corridor" approach. Predictive displays have shown effectiveness in compensating for delays and enhancing vehicle mobility in human-in-the-loop experiments [35], [36], [37], [38], [39], [40], [41]. Predictive models can be model-based [38], model-free [40], or a combination of both [41], each having specific

strengths and limitations. Combining both approaches improves operation, though not significantly. In good performing model-based prediction strategies, the Smith predictor control strategy is used, which was introduced by O.J. Smith in 1957 [42] for delays in chemical processes. We employ Smith predictor stategy in our article to compare it with SRPT vehicle teleoperation. In summary, predictive displays enable real-time vehicle control for human-in-loop teleoperation, but their effectiveness may decrease in the presence of strong disturbances such as low-adhesion roads or crosswinds, leading to asynchrony issues.

Shared control - Equipped with obstacle avoidance capabilities, shared control aims to enhance the safety of the ego vehicle and other road participants in real-time. Schimpe and Diermeyer [18] proposed an MPC-based shared steering control for obstacle avoidance, modeling obstacles as repulsive potential fields. Qiao et al. [19] developed a human-machine interaction model using Nash equilibrium-based non-cooperative games. Schitz et al. [20] introduced an MPC-based assistance approach in cruise control mode. Storms et al. [21] presented an MPC-based shared control system for static obstacle avoidance, while Saparia et al. [16] used predictive displays to mitigate latency and MPC-based shared control for obstacle avoidance. Shared control faces similar challenges to direct control, such as prediction inaccuracy in disturbances. But with a functional perception module, it effectively assists the operator in collision avoidance and enhances safety. However, a downside is the strict requirement of a functional perception module.

B. Previous Work

In our prior research [43], we introduced SRPT, a pose-based control strategy for vehicle teleoperation. The driver model at the control station considers the delayed vehicle pose from the remote vehicle and the known mission plan. The control station discretely transmits the intended vehicle pose (reference pose) at 30 Hz. On the remote vehicle side, the controller receives reference pose and optimizes for steer and speed commands. It accounts for actuator constraints and environmental disturbances, utilizing IMU sensors in the vehicle to sense environmental changes. In other work [44], we evaluated SRPT, where the human operator creates waypoints (reference poses) by steering the augmented lookahead vehicle (blue) outline using joystick steering (fig. 1).

C. Contribution of paper

This article focuses on assessing the performance improvement of the SRPT approach for vehicle teleoperation by comparing it with the Smith prediction strategy for a range of vehicle speeds (14–26 km/h). In the Smith prediction strategy, after predicting vehicle states, two types of driver models are assessed. One is the Lookahead driver model and second is the Stanley driver model. The test track consists of maneuvers with progressively increasing difficulty. The experiments are performed in a Simulink simulation environment, where variable network delays (250–350 ms) and a 14-dof vehicle model for the main vehicle are considered.
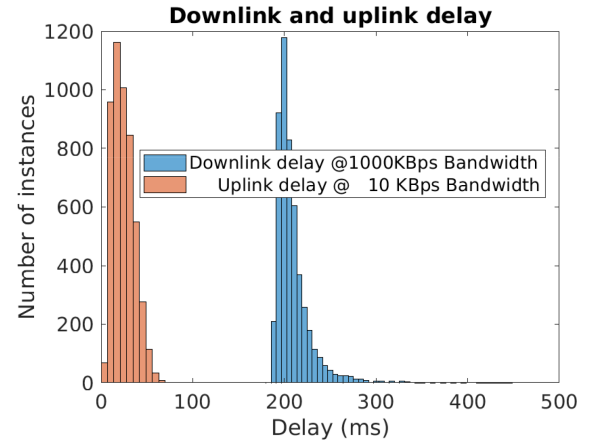

Fig. 3.   Delays observed in data transmission over 4G [43].

Overall, our experiments show that the SRPT approach outperforms the Smith prediction strategy in terms of accuracy, and stability, especially for challenging maneuvers. These findings demonstrate the potential of the SRPT approach to improve the safety and efficiency of vehicle teleoperation in real-world applications.

D. Outline of paper

The rest of the article is organized as follows. Section II-A presents the characteristics of network delay. Section II-B presents the Smith predictor with two driver models. Section II-C explains the SRPT mode. Section III provides an overview of the simulation platform. Section IV discusses the experimental structure. Section V presents and discusses the results. Section VI concludes with the work summary, key findings, and future work.

II. METHOD

A. Network Delays

The time delay involved in vehicle teleoperation can be divided into two parts from the perspective of the control station. The first part is termed as the downlink delay (τ_2), which pertains to the time taken for streamed images to reach the control station. The second part is referred to as the uplink delay (τ_1), encompassing the interval between generating driving commands at the control station and their execution in the vehicle. The downlink delay amalgamates several factors, including camera exposure delay, image encoding time, network transmission delay, and image decoding time, with network delay being the primary variable component.

In contrast, the uplink delay comprises the network transmission delay of driving commands to the vehicle and the subsequent vehicle actuation delay. In scenarios involving wireless communication via 4G, variability impacts both downlink and uplink delays. Fig. 3 displays the corresponding delays for the utilized bandwidth. This illustration considers 5000 picture frames and driving commands in a typical urban environment, with the vehicle connected to 4G mobile connectivity and the control station linked to wired internet.
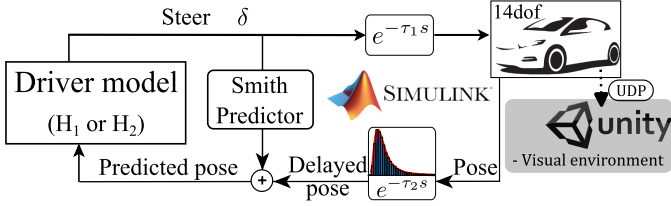
Fig. 4. Smith predictor schematic for vehicle teleoperation simulation. H_1 and H_2 are types of driver models considered. Unity has no role in simulation, it is just to display the manoeuvres.

Measurement of τ_1 occurs at the vehicle by subtracting the timestamp of driving commands from the current timestamp, while τ_2 is determined at the control station by subtracting the timestamp of a received image from the current timestamp.

B. Smith Predictor With Two Types of Driver Model

The Smith predictor approach [42] is a popular predictive control method used in bilateral teleoperation. It was first introduced by O.J. Smith in 1957 and is a model-based prediction approach. Fig. 4 shows a schematic of the Smith predictor in the control loop of vehicle teleoperation systems with variable time delays. The steering input is passed through the Smith predictor block, which outputs a correction term which needs to be added to the (received) delayed pose to predict the current pose of the vehicle. Smith predictor block is further elaborated in our previous work [43], where its transfer function is presented. It provides the human operator with the sense of controlling the vehicle in real-time by predicting the current position of the vehicle, bypassing the network delay. Thereupon, the human operator can steer based on vehicle current pose and the mission plan. In this article, two types of driver model are considered instead of human volunteers for the sake of reproducibility of results and as a preliminary comparison of the SRPT approach with the Smith predictor approach. Christoph Popp et al. [45] suggest that geometry base lateral controller for a vehicle works well for low lateral acceleration scenarios. Considering low-medium speed vehicle teleoperation, below mentioned two driver models are adopted.

1) Lookahead Driver, H_1: This driver model represents the general control tendency while driving at low-medium lateral accelerations, in which the human operator steers the vehicle to try to align a look-ahead point with the desired trajectory (Fig. 5(a)). Look-ahead driver model based on the cross-track error at the look-ahead point (motivated by [46]) is given by

$$\delta = -k_1 \cdot \Delta y_L \qquad (1)$$

$$lookahead\ Distance = \ k_2 \cdot V_x \ . \qquad (2)$$

δ : Steer angle.

k_1 : Gain term, a constant for a given vehicle longitudinal speed.

Δy_L : Cross-track error of the look-ahead point from the reference trajectory.
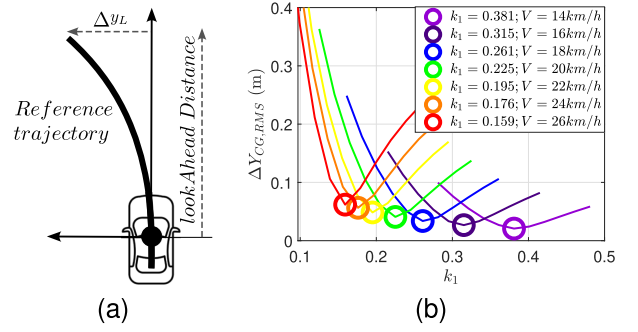
$k_2 = 0.90$: look-ahead time.

Fig. 5. (a) Look-ahead driver model control. (b) Tuning of k_1 for the look-ahead driver model by optimizing for minimum cross-track error in region-A keeping $k_2 = 0.9\,\mathrm{s}$ constant.
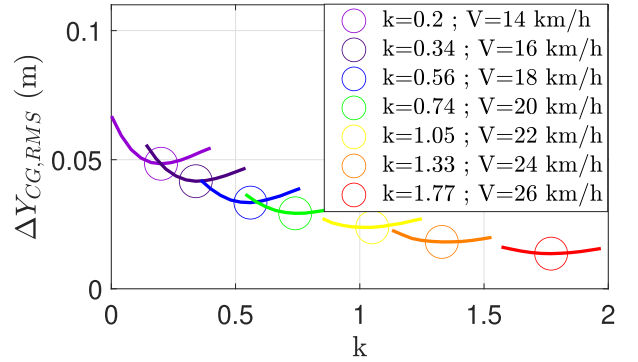

Fig. 6. Tuning of k for the Stanley controller by optimizing for minimum cross-track error in region-A.

k_1 is tuned for a range of vehicle speeds to have minimum deviation of vehicle (CG) from the reference trajectory, while driving across region-A of the trajectory shown in Fig. 9. Observations are presented in Fig. 5(b).

k_1 is tuned for a constant k_2 without considering network delays in the control loop. Although in the presence of delays a human operator can adapt his actions, but keeping $[k_1;\ k_2]$ unchanged ensures no adaptability and highlights performance deterioration due to delays.

2) Stanley Lateral Controller Driver, H_2: Kinematic Stanley controller [47] with the reference point at center of front axle, given by

$$\delta = \begin{cases} \Delta\psi + \tan^{-1}\frac{k\Delta y_F}{V_x} & \text{if } \left|\Delta\psi + \tan^{-1}\frac{k\Delta y_F}{V_x}\right| < \delta_{\max} \\ \delta_{\max} & \text{if } \Delta\psi + \tan^{-1}\frac{k\Delta y_F}{V_x} \geq \delta_{\max} \\ -\delta_{\max} & \text{if } \Delta\psi + \tan^{-1}\frac{k\Delta y_F}{V_x} \leq -\delta_{\max} \end{cases} \qquad (3)$$

$\Delta\psi$ represents the vehicle's heading relative to the nearest segment of the trajectory. The variable Δy_F represents the cross-track error at the front axle center. V_x represents the vehicle speed. k is also tuned for the same range of vehicle speeds to have minimum deviation of vehicle (CG) from the reference trajectory while driving across region-A of the same trajectory. Observations are presented in Fig. 6.

Parameters of both driver models are tuned in only region-A of the trajectory. Region-A is not constant radius but it carries
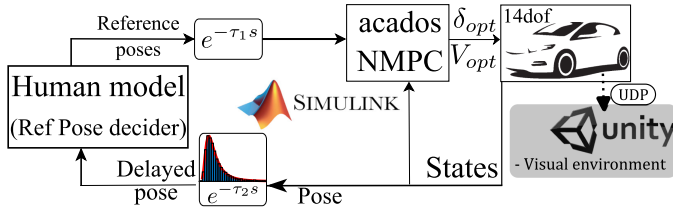
Fig. 7. SRPT schematic for vehicle teleoperation simulation. Unity has no role in simulation, it is just to display the manoeuvres.
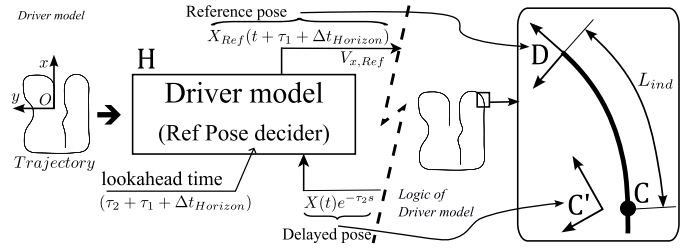

Fig. 8. Working principle of the reference-pose decider block. Its task is to choose the future reference pose based on the received vehicle pose and look-ahead distance.

variable curvature across itself as shown in Fig. 9. This means the driver models are tuned for variable curvatures.

C. SRPT Teleoperation Approach With Reference-Pose Decider Driver Model

In predictive display vehicle teleoperation, where the model-based prediction approach (discussed above) is effective on normal roads and under normal conditions. Disturbances like strong winds, low-adherence roads, and bumps can alter vehicle dynamics. Parameter estimation techniques presented in articles [48], [49] can be useful for changes in dynamics that last from medium to high duration. These techniques use sliding window batch estimation, the estimations itself are delayed (due to convergence time). Momentary disturbances can have a significant impact on the vehicle output before the new plant dynamics are estimated at the control station and corrective action is taken by the human operator.

The SRPT approach for vehicle teleoperation differs from traditional methods, in SRPT the human operator transmits reference poses instead of steer-throttle commands to the remote vehicle. These reference poses are generated with a look-ahead time of $[1 + \tau_1 + \tau_2]s$, which results in the vehicle receiving reference-poses approximately 1 s ahead of its current position. This horizon of 1 s is chosen arbitrarily based on the fact that a driver typically steers a vehicle based on upcoming vehicle position. The same time horizon of $\Delta t_{Horizon} = 1$ s is also used (inside vehicle) for the NMPC block to optimize for vehicle steer-speed commands. While the SRPT approach is effective, it represents a departure from conventional vehicle teleoperation, where the human operator transmits steer-throttle commands to the remote vehicle.

1) Reference-Pose Decider Driver Model: The task of the human model block is to transmit information that informs the vehicle about its aiming direction. Referring to Fig. 8, human model block receives delayed vehicle states, $X(t)e^{-\tau_2 s}$, which consists of vehicle pose, $P_O^{C'}$. It is the delayed vehicle pose in global reference frame, O. Being aware of the whole trajectory, the human model block first finds the closest point C on the reference trajectory. Then it finds the point D, which is L_{ind} distance ahead of point C. The L_{ind} is the look-ahead distance govern by below relation:

$$L_{ind} = V_x \cdot \tau + \max\left(V_x \cdot \Delta t_{Horizon}, \ l_F\right). \quad (4)$$

It is lower bounded by l_F, the front axle distance from CG. It is linearly proportional to the round trip delay ($\tau = \tau_1 + \tau_2$)

and to the vehicle speed (V_x). The first term tries to compensate for round-trip delay, and the second term aims to generate the terminal condition for the NMPC horizon. There are two ways in which the aiming direction can be transmitted to the vehicle:

1) Transmit the relative reference pose, $P_{C'}^D$. It is the relative position and heading of pose-D with respect to pose-C', it acts as a correction term, which tries to bring the vehicle close to the desired trajectory. Upon receive of this relative pose, the vehicle first estimates how much it has already traveled during the round-trip delay and how much more it has to travel. This estimation is possible, as messages are timestamped.

2) Transmit the global reference pose. Transmit the reference pose, X_{Ref}, in global reference frame.

$$X_{Ref} = P_O^{C'} + P_{C'}^D = P_O^D \quad . \quad (5)$$

For this article, we adopt the second approach, which does not require the vehicle to explicitly estimate how much it has travelled during the round-trip delay. Modeling this driver model for simulation is straightforward as the entire trajectory is pre-known. However, in human-in-the-loop experiments, an equivalent driver model can be obtained, where the correction, $P_{C'}^D$, can be decided by the human operator. In our previous work [44], this correction term is getting generated online using a steering joystick, briefly represented by the below relation

$$X_{Ref} = P_O^{C'} + \Delta P_{Joystick} \quad . \quad (6)$$

$\Delta P_{Joystick}$ - It is the correction term generated by the augmented lookahead vehicle (blue) outline on the visual interface (Fig. 1) with help of joystick steering.

D. NMPC Block

The NMPC block on the vehicle side takes into account the reference poses received, it analyzes the current states of the vehicle, and actuator constraints to generate optimized steer and speed commands. The prediction model of NMPC is presented in our previous work [43], [44]. The objective is to synchronize the target reference pose with the trajectory of the vehicle while minimizing inputs (steer-rate and vehicle acceleration) and maintaining a speed close to the reference speed (V_{Ref}) asked by the human operator. It also respects input constraints. One input constraint is the maximum steer-rate of $360°/s$, which

TABLE I
14-DOF MODEL: VEHICLE BRIEF CHARACTERISTICS

Parameter	Value
m	1681 kg
I_z	2600 kg s^2
$[m_F;\ m_R]$	[871.6; 809.4] kg
$[l_F;\ l_R]$	[1.3; 1.4] m

TABLE II
DESCRIPTION OF THE BLOCKS USED IN THE SIMULATION PLATFORM

Block	Description	Rate
Vehicle 14dof	A 14dof vehicle model to simulate a real vehicle	1000 Hz
$e^{-\tau_2 s}$	Variable network downlink delay	30 Hz
Human model	Ref Pose decider driver	30 Hz
$e^{-\tau_1 s}$	Constant network uplink delay $\tau_1 = 0.060s$	30 Hz
NMPC	Non-linear model predictive controller Acados toolkit	50 Hz
Unity	An external block, to visualize the real vehicle maneuvers	100 Hz

is due to the actuator constraint of the motor for the steering actuation. Another input constraint is vehicle acceleration and deceleration limits. Further description of NMPC block is presented in the previous works mentioned earlier. A prediction horizon ($\Delta t_{Horizon}$) of 1 s is used, divided into 50 intervals through discrete multiple shooting, and solved by sequential quadratic programming with the real-time NMPC solver ACADOS [50], [51].

III. SIMULATION PLATFORM

A faster than real-time simulation test platform for vehicle teleoperation with network delay is developed using Simulink + Unity3D, shown in Figs. 4 and 7. Unity3D is used only to provide visuals of vehicle maneuvers.

Table I provides a brief description of the vehicle type used in the 14-dof Simulink vehicle model, which represents a typical FWD passenger vehicle. Table II provides additional descriptions of each block, including their working rate.

The $e^{-\tau_2 s}$, Human model, and $e^{-\tau_1 s}$ blocks work synchronously with each other at 30 Hz to simulate the usual discrete nature of video streaming to the control station. The downlink delay (τ_2) is considered a variable delay to simulate usual network delays, while the uplink delay (τ_1) is considered a constant of 0.060 s due to its lower magnitude and variability. To simulate the downlink delay, a generalized extreme value distribution, $GEV(\xi = 0.29, \mu_{GEV} = 0.200, \sigma = 0.009)$ is used [38], [41]. Positive ξ means that the distribution has a lower bound of $(\mu_{GEV} - \frac{\sigma}{\xi}) \approx 0.169$ s (> 0) and a continuous right tail based on extreme value theory, keeping the variable downlink delay in the range of $0.169\,s - 0.300$ s.

IV. EXPERIMENTAL SETUP

Fig. 9 shows a 438 m test track consisting of eight regions labeled from A to H. These regions simulate increasingly challenging maneuvers and severe environmental conditions. Region A involves cornering with a radius of 15 m ($R15$), B involves
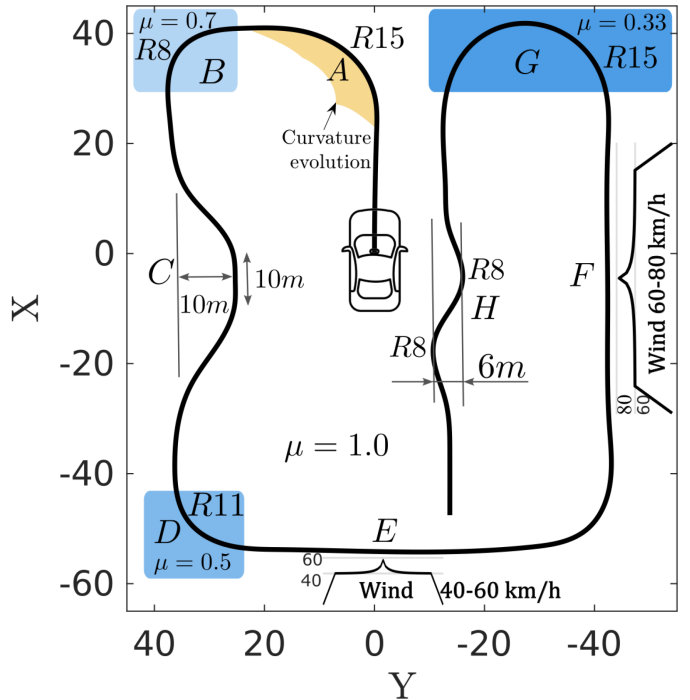

Fig. 9. Track contains various sections A–H of difficult manoeuvres and worst-case environmental conditions.

cornering ($R8$) on a surface with road adherence coefficient of $\mu = 0.7$. Region C is double lane change, D involves cornering with $\mu = 0.5$, E-F includes strong lateral wind with a Chinese hat profile [52], [53], G involves a U-turn with $\mu = 0.33$, and H involves a slalom. All the curves have gradually changing curvature, as shown for region-A. The objective is to follow the track centerline as closely as possible, with a maximum vehicle speed limit of V_{Ref}, specified by the human block. It is anticipated that during difficult manoeuvres, the NMPC block regulates the vehicle speed (V_{opt}) to minimize the cross-track error, which is a desirable behavior.

To compare SRPT performance over Smith-predictor performance, a total of eight modes are considered (as given below):
1. NoDelay -LookAhead driver
2. Delay -LookAhead driver
3. Delay -LookAhead driver (Smith)
4. NoDelay - Stanley driver
5. Delay - Stanley driver
6. Delay - Stanley driver (Smith)
7. NoDelay - RefPoses driver (SRPT)
8. Delay - RefPoses driver (SRPT)

Also, to assess performances over a range of vehicle speeds, each mode is tested on vehicle speeds ranging from $V_{Ref} = 14$ km/h to $V_{Ref} = 26$ km/h in succession.

V. RESULTS AND DISCUSSION

The extent of performance degradation due to delays is expected to vary based on the vehicle speed and path difficulty (tight corners). At lower speeds, latency effects are less
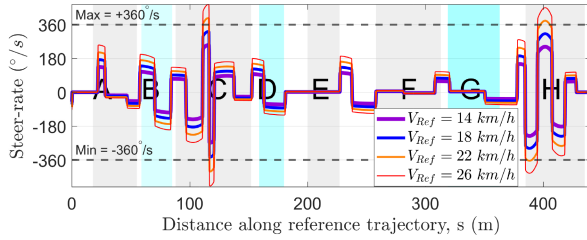
Fig. 10. Approximate steer-rate requirement for the track for various vehicle speeds. (This figure provides a preliminary indication of the anticipated challenges during evaluations at higher vehicle speeds.).

pronounced as the human operator has more time to correct the maneuver and vehicle has more time to respond to commands.

As speed increases, the available response time to perform a maneuver decreases, and latency can significantly impact the accuracy and safety of the maneuver. The chosen test track has an increasing level of difficulty along its length and it will get traversed at various speeds, one at a time, for this study. Just to understand the approximate steer-rate requirement for the track at corresponding vehicle speeds, the Ackermann steering relation can be used as given below:

$$\delta(s) = \tan^{-1}\left[\frac{L}{R(s)}\right] \quad (7)$$

$$steer\ rate, \frac{d\delta}{dt}(s) = \frac{d\delta}{ds} \cdot \frac{ds}{dt} = \frac{d\delta}{ds} \cdot V \quad (8)$$

$\delta(s)$: Steer angle.
L : Wheelbase.
$R(s)$: Radius of curvature along the track length (s).
V : Vehicle speed.

In Fig. 10, the steer-rate requirement for different vehicle speeds along the track is shown. It can be observed that in regions C and H, the steer-rate requirement exceeds the steer-rate capability of the steering motor for reference speeds ≥ 22 km/h. This indicates that, at elevated speeds, the vehicle might struggle to execute essential steering maneuvers, potentially resulting in increased cross-track error and diminished performance. Given that the track encompasses factors beyond steer-rate constraints that can adversely affect performance, we have chosen to use cross-track error as the performance metric, aiming for its minimization. Cross-track error is defined as the minimum Euler distance between the vehicle CG and the reference path at any given time. The RMS of the cross-track error at the vehicle's CG is computed for each track region to facilitate a performance comparison among the respective vehicle teleoperation modes.

Fig. 11 presents a quantitative analysis of cross-track errors observed in regions A-H for different vehicle speeds and teleoperation modes. In region A-D, the Smith predictor ameliorates the negative effect of delays and tries to reduce the cross-track error to its respective undelayed mode (the green bars are shorter than the red bars). However, the SRPT mode, even with delay (purple bars), resulted in significantly smaller cross-track errors. In regions E-F with strong crosswinds, the Smith predictor approach results in larger cross-track errors because it is unaware of the wind disturbances. In contrast, the NMPC controller in the
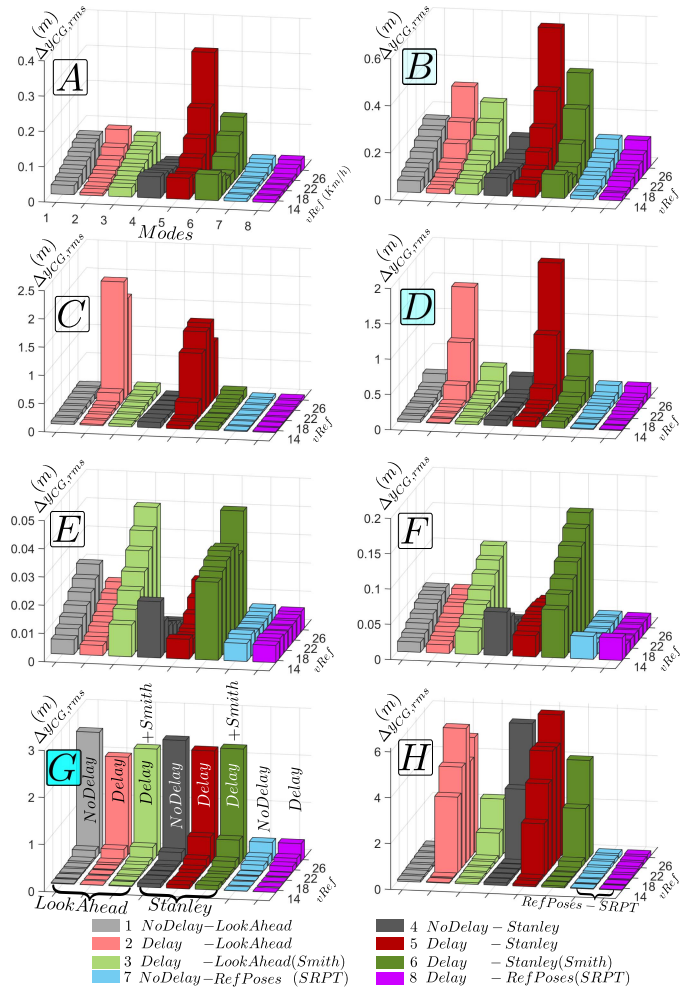

Fig. 11. Vehicle teleoperation simulation result on the metric of cross-track error (Δy_{CG}) with various modes for vehicle speeds $14 - 26$ km/h. SRPT vehicle teleoperation is found to be accurately tracing the track, even in the presence of variable delays.

SRPT mode takes vehicle states as input, leading to a significant improvement in teleoperation. In region-G ($\mu = 0.33$), for the high-speed lap, all teleoperation modes except the SRPT mode resulted in high lateral slip and therefore high cross-track errors. In region-H (the slalom), the cumulative impact of both the steer-rate constraint and delay in the control loop deteriorates the performance. Even in this region, the SRPT mode demonstrated a significant reduction in cross-track error.

The analysis of the results revealed that the primary reason for the superior tracking performance of the SRPT mode is its ability to moderate the vehicle speed appropriately in areas where it is necessary to minimize the cross-track error. Consequently, this leads to a slight increase in the completion time, as shown in Fig. 12. An example of the trade-off between completion time and safety can be seen in region-H (slalom) where SRPT mode resulted in a 25% increase in completion time at $V_{Ref} = 26$ km/h. Despite the longer completion time, this mode ensures higher safety and minimizes cross-track error, which is particularly important for this tight slalom at this vehicle speed.
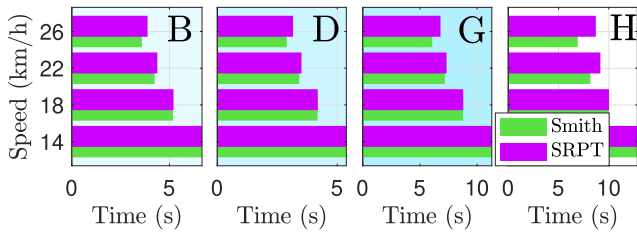
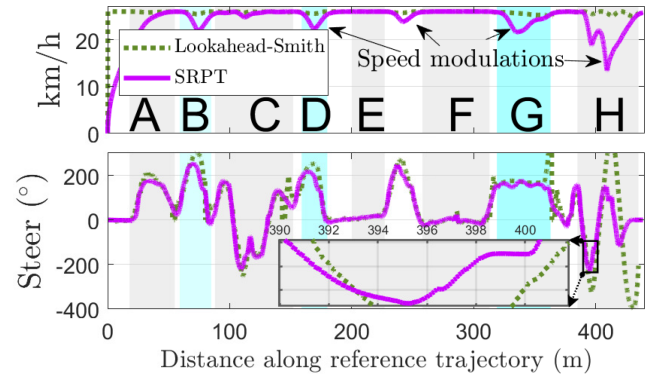Fig. 12. Completion time comparison SRPT vs Smith mode for [B,D,G,H] regions.

Fig. 14. Evolution of speed and steer profile for Lookahead-Smith and SPRT mode under variable delays. Automatic speed reduction is evident in SRPT mode, this allows more time to steer in tight cornering regions.

Fig. 14 shows the vehicle speed profile along the track length for Lookahead-Smith mode and SRPT mode, both in the presence of network delays. The SRPT mode implemented automatic speed modulations, which were noticeable in all cornering regions, particularly in the slalom region. These modulations helped steer in advance, as shown in the zoomed rectangle inside the figure.

Interestingly, the performance of the SRPT mode, with and without network delay, is similar (blue bars and purple bars are similar in height in Fig. 11). This can be attributed to the difference in SRPT mode operating principle, wherein the vehicle receives reference poses instead of steer commands from the control station.

A. Discussion on Implications of Network Routing and Network Discontinuity

In a real-world scenario, the vehicle is mobile and can be connected through 4G/5G networks. On the other hand, the control station, being a static entity, can be linked to a high-speed wired internet connection, as lower latency enhances safety. The delays experienced in network communication might be influenced not only by the inherent network characteristics but also by routing choices made between different network operators' systems (inter-domain) and within a single organization's network (intra-domain). In our latency measurement experiments, we used two distinct network operators.

To maintain the broad applicability of our work, we considered lumped forms of downlink and uplink delays. Specifically, the lumped downlink delay is essentially the location-shifted distribution of the variable network delay part. The variable network delay distribution is well-fitted using the generalized extreme value (GEV) distribution with parameters including location, scale, and shape.

The challenge of unreliable connectivity in 4G/5G networks is a tangible concern. For the scope of this work, we have chosen not to merge the issue of extreme network discontinuity, as unreliable connectivity can lead to substantially greater delays. This concern demands a distinct approach, possibly involving measures such as emergency stop mechanisms, the introduction
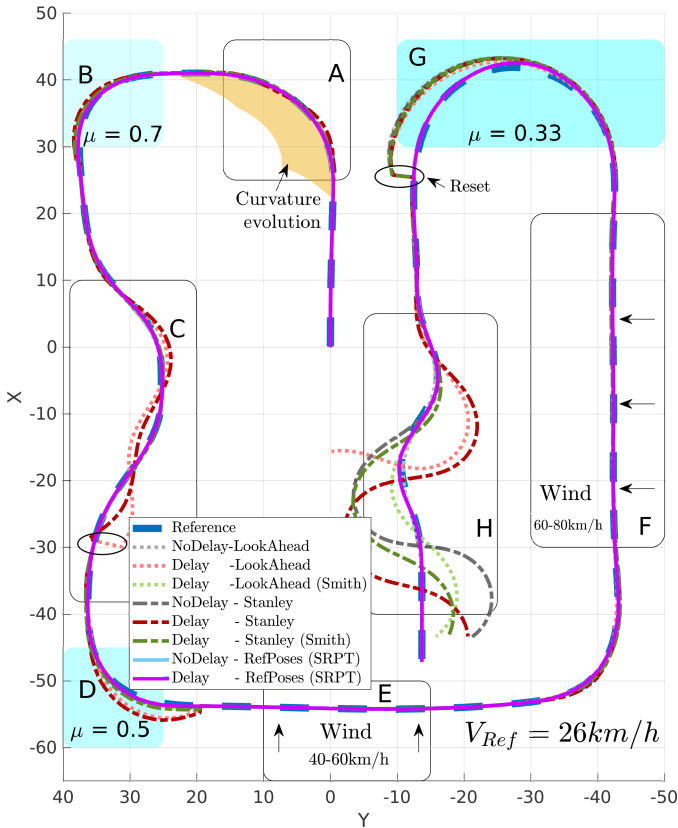

Fig. 13. Vehicle teleoperation simulation result with various modes at $V_{Ref} = 26$ km/h. SRPT vehicle teleoperation accurately traces the track, even in the presence of variable delays.

Fig. 13 presents the trajectory traversed with all the teleoperation modes for $V_{Ref} = 26$ km/h. It qualitatively shows better performance of SRPT approach even in the presence of all the disturbances and variable delays. The red trajectory of look-ahead driver model resulted in big oscillations due to network delay and due to steer-rate saturation. If any mode deviates significantly from the track, to the extent that it may compromise the results of the subsequent region, the mode is reset before entering the new region, while maintaining the vehicle's initial speed as the reference speed.

These large deviations and oscillations are not present in SRPT approach because NMPC block accounts for the steer-rate limitation and subsequently decelerates the vehicle to allow for more time to steer.

of full autonomy for safe parking, or the implementation of redundant internet connections. Addressing this challenge is crucial to ensuring the robustness and reliability of vehicle teleoperation, especially in scenarios where network connectivity might be compromised.

VI. CONCLUSION

In this article, we evaluated the SRPT approach for vehicle teleoperation, which involves transmitting reference poses to the remote vehicle instead of steering commands. A simulation framework was established in a Simulink environment to assess the approach under variable network delays (250–350 ms). We compared the performance of SRPT with the Smith predictor approach, incorporating two driver models: Lookahead and Stanley. Our simulation experiments encompassed diverse maneuvers and vehicle speeds ($V_{Ref} = 14$–26 km/h), with the performance index being the RMS of cross-track error across various sections of the test track.

The findings demonstrated the effectiveness of the SRPT approach across all maneuvers and environmental disturbances, for a range of vehicle speed. It consistently exhibited lower cross-track error compared to other teleoperation modes. Notably, SRPT excelled in path tracking performance, particularly in challenging scenarios such as low-adhesion road and slalom regions, showcasing significant improvement compared to other modes. The inherent mechanism of the SRPT approach allowed adaptive vehicle speed moderation during critical moments, granting additional time for steering during maneuvers. Although this led to a slight increase in completion time for complex maneuvers, the SRPT approach remained robust despite network delays.

For real-world deployment, integrating a state estimator within the vehicle becomes essential. As we look ahead, investigating the effect of network routing on delays and exploring the impact of state-estimation inaccuracies on SRPT performance are vital directions for future research. Ultimately, this framework is poised for implementation in actual vehicle teleoperation experiments, bridging the gap between simulation and practical application.

REFERENCES

[1] D. Majstorovic, S. Hoffmann, F. Pfab, A. Schimpe, M.-M. Wolf, and F. Diermeyer, "Survey on teleoperation concepts for automated vehicles," in *Proc. IEEE Int. Conf. Syst., Man, Cybernet.*, 2022, pp. 1290–1296, doi: 10.1109/smc53654.2022.9945267.

[2] D. Bogdoll, S. Orf, L. Töttel, and J. M. Zöllner, "Taxonomy and survey on remote human input systems for driving automation systems," in *Proc. Future Inf. Commun. Conf.*, 2022, pp. 94–108, doi: 10.1007/978-3-030-98015-3_6.

[3] O. Amador, M. Aramrattana, and A. Vinel, "A survey on remote operation of road vehicles," *IEEE Access*, vol. 10, pp. 130135–130154, 2022.

[4] J. Storms and D. Tilbury, "Equating user performance among communication latency distributions and simulation fidelities for a teleoperated mobile robot," in *Proc. IEEE Int. Conf. Robot. Automat.*, 2015, pp. 4440–4445.

[5] J. P. Luck, P. L. McDermott, L. Allender, and D. C. Russell, "An investigation of real world control of robotic assets under communication latency," in *Proc. 1st ACM SIGCHI/SIGART Conf. Hum.-Robot Interaction*, 2006, pp. 202–209.

[6] T. B. Sheridan, "Space teleoperation through time delay: Review and prognosis," *IEEE Trans. Robot. Automat.*, vol. 9, no. 5, pp. 592–606, Oct. 1993.

[7] D. J. Gorsich, P. Jayakumar, M. P. Cole, C. M. Crean, A. Jain, and T. Ersal, "Evaluating mobility performance of unmanned ground vehicles," US ARMY TARDEC WARREN United States, Warren, MI, USA, Tech. Rep. 29559, 2018.

[8] J.-M. Georg, J. Feiler, S. Hoffmann, and F. Diermeyer, "Sensor and actuator latency during teleoperation of automated vehicles," in *Proc. IEEE Intell. Veh. Symp.*, 2020, pp. 760–766.

[9] C. Mutzenich, S. Durant, S. Helman, and P. Dalton, "Updating our understanding of situation awareness in relation to remote operators of autonomous vehicles," *Cogn. Res.: Princ. Implic.*, vol. 6, no. 1, Feb. 2021, Art. no. 9, doi: 10.1186/s41235-021-00271-8.

[10] S. Hoffmann and F. Diermeyer, "Systems-theoretic safety assessment of teleoperated road vehicles," in *Proc. 7th Int. Conf. Veh. Technol. Intell. Transport Syst.*, 2021, pp. 446–456.

[11] F. E. Chucholowski, "Evaluation of display methods for teleoperation of road vehicles," *J. Unmanned Syst. Technol.*, vol. 3, no. 3, pp. 80–85, 2016.

[12] T. Tang, P. Vetter, S. Finkl, K. Figel, and M. Lienkamp, "Teleoperated road vehicles the "free corridor" as a safety strategy approach," *Appl. Mechanics Mater.*, vol. 490, pp. 1399–1409, Jan. 2014, doi: 10.4028/www.scientific.net/amm.490-491.1399.

[13] G. Graf et al., "The predictive corridor: A virtual augmented driving assistance system for teleoperated autonomous vehicles," in *Proc. Int. Conf. Artif. Reality Telexistence Eurographics Symp. Virtual Environments*, 2020, pp. 61–69.

[14] J.-M. Georg and F. Diermeyer, "An adaptable and immersive real time interface for resolving system limitations of automated vehicles with teleoperation," in *Proc. IEEE Int. Conf. Syst., Man Cybernet.*, 2019, pp. 2659–2664, doi: 10.1109/SMC.2019.8914306.

[15] J.-M. Georg, E. Putz, and F. Diermeyer, "Longtime effects of videoquality, videocanvases and displays on situation awareness during teleoperation of automated vehicles*," in *Proc. IEEE Int. Conf. Syst., Man, Cybern.*, 2020, pp. 248–255, doi: 10.1109/SMC42975.2020.9283364.

[16] S. Saparia, A. Schimpe, and L. Ferranti, "Active safety system for semi-autonomous teleoperated vehicles," in *Proc. IEEE Intell. Veh. Symp. Workshops*, 2021, pp. 141–147.

[17] S. J. Anderson, S. B. Karumanchi, K. Iagnemma, and J. M. Walker, "The intelligent copilot: A constraint-based approach to shared-adaptive control of ground vehicles," *IEEE Intell. Transp. Syst. Mag.*, vol. 5, no. 2, pp. 45–54, Summer 2013.

[18] A. Schimpe and F. Diermeyer, "Steer with me: A predictive, potential field-based control approach for semi-autonomous, teleoperated road vehicles," in *Proc. IEEE 23rd Int. Conf. Intell. Transp. Syst.*, 2020, pp. 1–6.

[19] B. Qiao, H. Li, and X. Wu, "Intelligent-assist algorithm for remote shared-control driving based on game theory," *J. Shanghai Jiaotong Univ. (Science)*, vol. 26, no. 5, pp. 615–625, Oct. 2021, doi: 10.1007/s12204-021-2351-z.

[20] D. Schitz, G. Graf, D. Rieth, and H. Aschemann, "Model-predictive cruise control for direct teleoperated driving tasks," in *Proc. Eur. Control Conf.*, 2021, pp. 1808–1813.

[21] J. Storms, K. Chen, and D. Tilbury, "A shared control method for obstacle avoidance with mobile robots and its interaction with communication delay," *Int. J. Robot. Res.*, vol. 36, no. 5-7, pp. 820–839, 2017, doi: 10.1177/0278364917693690.

[22] S. Gnatzig, F. Schuller, and M. Lienkamp, "Human-machine interaction as key technology for driverless driving - a trajectory-based shared autonomy control approach," in *Proc. IEEE RO-MAN: 21st IEEE Int. Symp. Robot Hum. Interactive Commun.*, 2012, pp. 913–918.

[23] S. Hoffmann, D. Majstorović, and F. Diermeyer, "Safe corridor: A trajectory-based safety concept for teleoperated road vehicles," in *Proc. Int. Conf. Connected Veh. Expo*, 2022, pp. 1–6.

[24] J. S. Kay and C. E. Thorpe, "Operator interface design issues in a low-bandwidth and high-latency vehicle teleoperation system," in *Proc. Int. Conf. Environ. Syst.*, SAE International, Jul. 1995, doi: 10.4271/951485.

[25] A. Björnberg, "Shared control for vehicle teleoperation with a virtual environment interface," Master's thesis, KTH, School of Electrical Engineering and Computer Science (EECS), Stockholm, Sweden, 2020.

[26] D. Schitz, G. Graf, D. Rieth, and H. Aschemann, "Interactive corridor-based path planning for teleoperated driving," in *Proc. IEEE 7th Int. Conf. Mechatronics Robot. Eng.*, 2021, pp. 174–179, doi: 10.1109/icmre51691.2021.9384848.

[27] A. Hosseini, T. Wiedemann, and M. Lienkamp, "Interactive path planning for teleoperated road vehicles in urban environments," in *Proc. 17th Int. IEEE Conf. Intell. Transp. Syst.*, 2014, pp. 400–405.

[28] D. Schitz, S. Bao, D. Rieth, and H. Aschemann, "Shared autonomy for teleoperated driving: A real-time interactive path planning approach," in *Proc. IEEE Int. Conf. Robot. Automat.*, 2021, pp. 999–1004.

[29] J. Feiler and F. Diermeyer, "The perception modification concept to free the path of an automated vehicle remotely," in *Proc. 7th Int. Conf. Vehicle Technol. Intell. Transp. Syst. Sci. Technol.,* 2021, pp. 405–412, doi: 10.5220/0010433304050412.

[30] M. Hofbauer, C. B. Kuhn, G. Petrovic, and E. Steinbach, "TELECARLA: An open source extension of the CARLA simulator for teleoperated driving research using off-the-shelf components," in *Proc. IEEE Intell. Veh. Symp.*, 2020, pp. 335–340.

[31] A. Schimpe, J. Feiler, S. Hoffmann, D. Majstorović, and F. Diermeyer, "Open source software for teleoperated driving," in *Proc. Int. Conf. Connected Veh. Expo*, 2022, pp. 1–6.

[32] I. Jatzkowski et al., "Integration of a vehicle operating mode management into UNICARagil's automotive service-oriented software architecture," 2021. [Online]. Available: https://leopard.tu-braunschweig.de/receive/dbbs_mods_00069881

[33] 5GCroCo, "Deliverable d2.2: Test case definition and test site description for second round tests and trials" Fifth Generation Cross-Border Control, Tech. Rep. 825050, Oct. 2021.

[34] F. Chucholowski, S. Büchner, J. Reicheneder, and M. Lienkamp, "Prediction methods for teleoperated road vehicles," in *Proc. Conf. Future Automot. Technol. - Focus Electromobility*, Garching bei München, Germany, Jan. 2013.

[35] F. Chucholowski, "Evaluation of display methods for teleoperation of road vehicles," *J. Unmanned Syst. Technol.*, vol. 3, pp. 80–85, 2016.

[36] A. Hosseini, F. Richthammer, and M. Lienkamp, "Predictive haptic feedback for safe lateral control of teleoperated road vehicles in urban areas," in *Proc. IEEE 83rd Veh. Technol. Conf.*, 2016, pp. 1–7.

[37] M. J. Brudnak, "Predictive displays for high latency teleoperation," in *Proc. NDIA Ground Veh. Syst. Eng. Technol. Symp.*, 2016, pp. 1–16.

[38] J. Prakash, M. Vignati, E. Sabbioni, and F. Cheli, "Predictive display with perspective projection of surroundings in vehicle teleoperation to account time-delays," *IEEE Trans. Intell. Transp. Syst.*, vol. 24, no. 9, pp. 9084–9097, Sep. 2023.

[39] T. Chen, "Methods for improving the control of teleoperated vehicles," Ph.D. dissertation, Technical University of Munich, Munich, Germany, 2015.

[40] Y. Zheng, M. J. Brudnak, P. Jayakumar, J. Stein, and T. Ersal, "A delay compensation framework for predicting heading in teleoperated ground vehicles," *IEEE/ASME Trans. Mechatronics*, vol. 24, no. 5, pp. 2365–2376, Oct. 2019.

[41] Y. Zheng, M. J. Brudnak, P. Jayakumar, J. L. Stein, and T. Ersal, "Evaluation of a predictor-based framework in high-speed teleoperated military ugvs," *IEEE Trans. Human-Mach. Syst.*, vol. 50, no. 6, pp. 561–572, Jun. 2020.

[42] J. M. Smith, "Closer control of loops with dead time," *Chem. Eng. Prog.*, vol. 53, pp. 217–219, 1957.

[43] J. Prakash, M. Vignati, E. Sabbioni, and F. Cheli, "Vehicle teleoperation: Successive reference-pose tracking to improve path tracking and to reduce time-delay induced instability," in *Proc. IEEE Veh. Power Propulsion Conf.*, 2022, pp. 1–8.

[44] J. Prakash, M. Vignati, E. Sabbioni, and F. Cheli, "Vehicle teleoperation: Human in the loop performance comparison of Smith predictor with novel successive reference-pose tracking approach," *Sensors*, vol. 22, no. 23, 2022, Art. no. 9119.

[45] C. Popp, C. Ziegler, M. Sippel, and H. Winner, "Ideal reference point in planning and control for automated car-like vehicles," *IEEE Trans. Intell. Veh.*, vol. 8, no. 2, pp. 1415–1424, Feb. 2023.

[46] J. Park and P. E. Nikravesh, "A look-ahead driver model for autonomous cruising on highways," *SAE Trans.*, vol. 105, pp. 1569–1577, 1996.

[47] G. M. Hoffmann, C. J. Tomlin, M. Montemerlo, and S. Thrun, "Autonomous automobile trajectory tracking for off-road driving: Controller design, experimental validation and racing," in *Proc. Amer. Control Conf.*, 2007, pp. 2296–2301.

[48] T. Teng and P. R. Grant, "Adaptive Smith predictor for teleoperation of UAVs using parameter estimation techniques," *AIAA Scitech Forum*, p. 1077, 2019.

[49] C. Thomas, S. Yi, S. Meadows, and R. Sherrill, "Adaptive smith predictor for teleoperation of UAVs with time-varying internet delay," *Int. J. Control, Automat. Syst.*, vol. 18, no. 6, pp. 1465–1473, 2020.

[50] R. Verschueren et al., "Towards a modular software package for embedded optimization," in *Proc. IFAC Conf. Nonlinear Model Predictive Control*, 2018, pp. 374–380.

[51] R. Verschueren et al., "acados–A modular open-source framework for fast embedded optimal control," *Math. Program. Computation*, vol. 14, no. 14, pp. 147–183, Oct. 2021, doi: 10.1007/s12532-021-00208-8.

[52] C. Baker, "Unsteady wind loading on a wall," *Wind Structures*, vol. 4, pp. 413–440, 2001.

[53] C. Baker, "Modelling of extreme wind gusts," 2020, [Online]. Available: https://profchrisbaker.com/2020/09/05/modelling-of-extreme-wind-gusts/

Jai Prakash received the M.S. degree in mechanical engineering in 2018 from the Politecnico di Milano, Milan, Italy, where he is currently working toward the Ph.D. degree with the Mechanical Engineering Department, Politecnico di Milano. His research interests include computer-vision, robotics, vehicle dynamics and vehicle teleoperation.

Michele Vignati (Member IEEE) received the master's degree and Ph.D. in mechanical engineering from the Mechanical Department, Politecnico di Milano, Milan, Italy, in 2013 and 2017, respectively, with thesis on control strategies for distributed powertrain of hybrid and electric vehicles. Since 2019, he has been a Senior Assistant Professor (RTDB) in the research field of applied mechanics. In particular, he focuses on mechanical systems dynamics and control applied in the automotive field of which he has more than 40 publications in international journals and conferences. In 2018 he was the recipient of the Best Paper Award for a paper presented at the AVEC18 international conference. He worked on tire dynamics and modeling in cooperation with Pirelli while in the last years he is working in autonomous driving field. His expertise goes from vehicle and tire dynamics to vehicle control systems and energy management.

Edoardo Sabbioni received the Ph.D. degree in mechanical systems engineering from the Department of Mechanical Engineering, Politecnico di Milano, Milan, Italy, in 2007. He is currently an Associate Professor with the Department of Mechanical Engineering, Politecnico di Milano. He is an author of more than 140 scientific publications, most of which published on peer-reviewed journals or presented at international conferences. His main research interests include stability, dynamics and control of mechanical systems, with applications to road and rail vehicles. He is also involved in research activities within the fields of aerodynamics and mechatronics. More in particular, he carried out numerical-experimental researches concerned with active safety of vehicles, design of control systems to improve vehicle handling and ride comfort, design of HiL (Hardware-in-the-Loop) test benches, electric and hybrid electric vehicles, autonomous and connected vehicle, smart tires technology, cross wind on road/rail vehicles. He is a member of the Editorial Board of Shock and Vibration. During his research activity, he cooperated and still cooperates with the main Italian automotive/railway industries and he was involved in several Italian and EC funded projects.